PAPER • **OPEN ACCESS**

Radiation exposure of astronauts following an intense solar particle event: analysis and comparison of doses in male and female voxel phantoms

IOP Publishing J. Radiol. Prot. 44 (2024) 041502 https://doi.org/10.1088/1361-6498/ad7ff6

Journal of Radiological Protection

OPEN ACCESS

RECEIVED
17 June 2024

REVISED
29 August 2024

ACCEPTED FOR PUBLICATION
26 September 2024

PUBLISHED
9 October 2024

PAPER

Radiation exposure of astronauts following an intense solar particle event: analysis and comparison of doses in male and female voxel phantoms

Ricardo Luis Ramos[1,*], **Elena Bernardini**[2], **Mario Carante**[1,3], **Alfredo Ferrari**[4], **Paola Sala**[5], **Valerio Vercesi**[1] and **Francesca Ballarini**[1,3]

[1] INFN, Sezione di Pavia, via Bassi 6, I-27100 Pavia, Italy
[2] Politecnico di Milano, Piazza Leonardo da Vinci 32, I-20133 Milano, Italy
[3] University of Pavia, Physics Department, Via Bassi 6, I-27100 Pavia, Italy
[4] Institute for Astroparticle Physics, Karlsruhe Institute of Technology, Karlsruhe, Germany
[5] Private, Thoiry, France
[*] Author to whom any correspondence should be addressed.

E-mail: ricardo.ramos@pv.infn.it

Keywords: solar particle events, space radiation protection, monte-carlo simulation, RBE, biophysical models

Abstract

According to NASA's plans, a human travel to the Moon is planned by the end of 2025 with the Artemis II mission, and humans should land on the Moon again in 2026. Exposure to space radiation is one of the main risks for the crew members; while for these short missions the doses from galactic cosmic rays would be relatively low, the possible occurrence of an intense solar particle event (SPE) represents a major concern, especially considering that in 2025 the Sun activity will be at its peak. Quantifying the amount and the effects of such exposure is therefore crucial, to identify shielding conditions that allow respecting the dose limits established by the various space agencies. By exploiting an interface between the BIANCA biophysical model and the FLUKA Monte Carlo radiation transport code, in this work we implemented a male and a female voxel phantom and we calculated absorbed doses and Gy-Eq doses in the various tissues/organs, as well as effective doses, following exposure to the August 1972 SPE, the most intense event of the modern era. The calculations were performed respect the organ dose limits for 30 d missions. A detailed comparison between male and female doses was then carried out, also considering that the Artemis II crew will include a woman. The results showed that female doses tend to be higher than male doses, especially with light shielding. This should be taken into account in mission design, also considering that, in a typical lunar mission, up to 15% of time may be spent in extra-vehicular activities, and thus with light shielding. More generally, this work outlines the importance of performing separate calculations for male and female astronauts when dealing with radiation doses and effects.

1. Introduction

Human space exploration has recently gained a renewed interest, also thanks to the fact that NASA is planning to go back to the Moon with the Artemis 2 mission by the end of 2025, and that the Moon may represent an intermediate step towards Mars (www.nasa.gov). Space radiation, which implies a continuous exposure to galactic cosmic rays (GCR) as well as occasional exposures to solar particle events (SPEs), has been classified as a 'red risk' for the crew members [1]. Since the maximum GCR dose-rate, which occurs during solar minimum periods, is in the order of 1 mSv d^{-1} [2], GCR exposure represents a serious hazard for the crewmembers of long-term missions. For instance, values in the range 0.30–0.45 Gy, that is 0.55–0.80 Gy-Eq or 0.87–1.20 Sv, have been estimated for a Mars mission [3], which should have an

Table 1. Organ dose limits with respect to non-cancer effects for missions of 30 d (30d), 1 year (1y) or for the whole astronaut career (car). The NASA limits were taken from [5], the ESA and RSA limits were taken from [6].

	NASA 30d (Gy-Eq)	ESA/RSA 30d (Sv)	NASA 1y (Gy-Eq)	ESA/RSA 1y (Sv)	NASA car. (Gy-Eq)	RSA car. (Sv)
Skin	1.5	1.5	3.0	3.0	6.0	6.0
Eye	1.0	0.5	2.0	1.0	4.0	2.0
BFO	0.25	0.25	0.5	0.5	—	—
Heart	0.25	—	0.5	—	1.0	—
CNS	0.5	—	1.0	—	1.5	—

approximate duration of two years. Furthermore, according to our previous work [4], the effective doses for a 650 d Mars mission at solar minimum would be lower than the 1 Sv career limit adopted by European Space Agency (ESA), but higher than the 600 mSv limit recently adopted by NASA. Lower doses may be involved for lunar missions: for instance, the doses for lunar operations of 1 year at solar minimum have been estimated to be in the range 0.10–0.12 Gy, corresponding to 0.18–0.22 Gy-Eq or 0.3–0.4 Sv [3].

Much lower GCR doses are expected for Artemis 2, which should have a duration of ten days. However, even for such a short mission, the risks due to a possible SPE cannot be neglected, especially considering that the Sun activity should be maximum in 2025. SPEs are occasional injections of high fluxes (up to more than 10^{10} particles/cm^2 in few hours) of protons and heavier charged particles coming from the Sun. These events are difficult to predict with appropriate timing, although it is known that the probability of an intense SPE is modulated by the Sun activity, which follows a 11 year cycle. Due to the high doses involved, intense SPEs represent a concern with respect to the so-called 'tissue reactions' (formerly called 'deterministic effects'), for which all space agencies have adopted dose limits for skin, eye and blood-forming organs (BFO). Furthermore, NASA also considered the heart and the central nervous system (CNS).

The limits for missions of different duration are reported in table 1 [5, 6]. Concerning skin, eye and BFO, while for skin and BFO the numbers are the same, for eyes the NASA values are higher than the ESA/RSA values by a factor of 2. However, a comparison is not straightforward because the NASA limits are expressed in Gy-Eq, by multiplying the absorbed dose in Gy by the relative biological effectiveness (RBE), whereas the ESA and RSA limits are expressed in Sieverts. In this framework, it is worth mentioning that space radiation RBE values are affected by large uncertainties [7], and that NCRP has indicated RBE fixed values for early, non-cancer effects [8]. These uncertainties are especially large for the CNS.

Such limits are applied to protect from non-cancer effects such as acute radiation syndrome (ARS) and degradation in crew performance, as well as for limiting cataracts, circulatory disease and CNS damage. In particular, the 30 d BFO limit is intended to protect against depletion of the hematopoietic system below a critical limit, as well as against nausea, vomiting and fatigue, which characterize the ARS prodromal phase. The 30 d skin limit should protect the skin from early (erythema and desquamation) and late (dermal atrophy, fibrosis, necrosis…) complications.

Several modelling works are available in the literature on the effects of SPEs e.g. [9–13]. Such works share the common philosophy of simulating the interactions of the different components of the SPE spectrum by means of an analytical or Monte Carlo radiation transport code. In general, the transport is first performed through an Al shield of variable thickness, and then in the human body. The latter is modelled by phantoms characterized by different levels of complexity, from simple water spheres to geometrical or voxel human phantoms that allow for a very realistic representation of the various tissues and organs. In many of these works, the absorbed dose is then multiplied by fixed RBE values to get tissue-specific Gy-Equivalent doses that can be compared with the corresponding limits.

NASA has adopted fixed RBE values for short term, non-cancer effects; such values depend on particle type but not on particle energy (except for neutrons) or dose. In a previous work [14] we have proposed a different approach, based on cell-survival RBE values calculated by means of the BIANCA biophysical model developed by our research group e.g. [15, 16]. This pragmatic choice relies on the idea that cell death is closely related to non-cancer effects: if the number of lost cells is large, observable harm occurs, reflecting the loss of tissue function [17]. Specifically, in that work BIANCA has provided particle- and energy-dependent linear and quadratic coefficients describing the dose-dependence of cell survival; afterwards, these coefficients have been read by the FLUKA Monte Carlo radiation transport code e.g. [18–20]. This has allowed calculating the dose-averaged linear and quadratic coefficients, as well as the corresponding RBE value, in each irradiated voxel. As a pilot study, this approach has been applied to calculate skin and BFO doses in a spherical water phantom following SPE exposure [14].

In the present work we extended the approach to a more realistic situation, by implementing a male and female human voxel phantom. Since it is known that the male and female body show a different response to

irradiation, a detailed comparison between male and female doses was carried out, also considering that a woman will be included in the Artemis 2 crew. As a sample SPE we considered the August 1972 event, which is regarded as the most intense event of the modern era.

2. Materials and methods

2.1. RBE calculation

BIANCA is a biophysical model that provides simulated dose-response curves for cell survival and chromosome aberration induction following irradiation by photons or by different monochromatic ion beams, up to Fe ions. The assumptions and parameters of the model, as well as the main simulation steps, have been described and discussed in detail in several publications e.g. [15, 16]. Herein, we will just mention that BIANCA relies on the idea that ionizing radiation induces a certain yield of DNA 'Critical Lesions' (CLs); a CL is defined as a severe DNA damage type that interrupts the continuity of the chromatin fiber producing two (main) independent chromatin fragments. These fragments either remain un-rejoined, or undergo distance-dependent incorrect rejoining, thus producing different types of chromosome aberrations; accidental correct rejoining is also allowed. Finally, some aberration types (dicentric chromosomes, rings and large deletions) are assumed to lead to cell death. As a first step, a radiobiological database consisting of the linear and quadratic coefficients describing the survival of V79 cells (chosen as a reference cell line) as a function of dose, ion type and energy has been produced [16]; afterwards, an algorithm has been developed to predict survival curves for, in principle, any other cell type [21]. In this work we applied the human skin fibroblast (HSF) database, which has been described in detail elsewhere [22]. Although, ideally, different, tissue-specific cell types should be used, we decided to use the HSF database both for skin and for the other tissue/organs. This pragmatic choice is related to the fact that much more systematic cell-survival data sets, for many different ion types and beam energies, are available in the literature for HSFs than for other (human) cell types. Furthermore, the photon alpha/beta ratio of 3.8 Gy resulting from the alpha and beta coefficients applied in this work ($\alpha = 0.17$ Gy^{-1}, $\beta = 0.045$ Gy^{-2}) is intermediate between early and late responding tissues.

In principle, the radiobiological tables produced by BIANCA can be read by any radiation transport code; like in previous works, also in the present work we used the FLUKA MC code, exploiting a pre-existing interface. Specifically, whenever according to FLUKA a certain dose, D_i, was deposited in a target voxel by a given radiation type, i (where 'radiation type' means a given particle of given energy), FLUKA read from the BIANCA tables the corresponding cell-survival coefficients (α_i and β_i), and used them to calculate the dose-averaged coefficients (α and β) describing the cell survival level due to the mixed radiation field in that voxel:

$$\alpha = \frac{\sum_{i=1}^{n} \alpha_i D_i}{\sum_{i=1}^{n} D_i} \quad \sqrt{\beta} = \frac{\sum_{i=1}^{n} \sqrt{\beta_i} D_i}{\sum_{i=1}^{n} D_i}.$$

Following calculation of these dose-averaged coefficients, the RBE in each voxel was calculated as D_x/D, where D is the total absorbed dose in the voxel, whereas D_X is the photon dose necessary to obtain the same biological effect, i.e. the same level of cell survival. A more detailed description of this method, which has been applied in several previous works in the framework of both cancer ion therapy and space radiation protection, can be found in previous publications [22–26].

2.2. FLUKA simulations

The SPE exposure of an astronaut inside a spacecraft in deep space was modelled by irradiating with FLUKA a female or a male phantom placed into a cylindrical Aluminium shielding with 38 cm radius, 180 cm height and variable thickness. The selected values for the Al thickness varied from 0.3 g cm^{-2} (light spacesuit) up to 20 g cm^{-2} (storm shelter), to simulate the necessary shielding in case of an intense SPE. The space between the shielding structure and the phantom was filled with air. An isotropic spherical source of 200 cm radius was implemented in the simulations. The spectrum of the August 1972 event was purposely implemented in this work. Figure 1 shows the particle differential flux for this event, according to the fitting of the proton, helium and oxygen spectra of the event reported in [27].

Thanks to the interface between BIANCA and FLUKA described in section 2.1, in addition to the absorbed dose in each voxel we also calculated the RBE value, and thus the Gy-Eq dose, in that voxel.

2.3. Phantom implementation and characteristics

In this work, the ICRP computational phantoms of the Reference Male and Reference Female described in [28] were implemented in FLUKA. These phantoms, which are based on medical imaging data of real people, were constructed after modifying the voxel models (Golem and Laura) of two individuals whose body height and mass resembled the reference data.

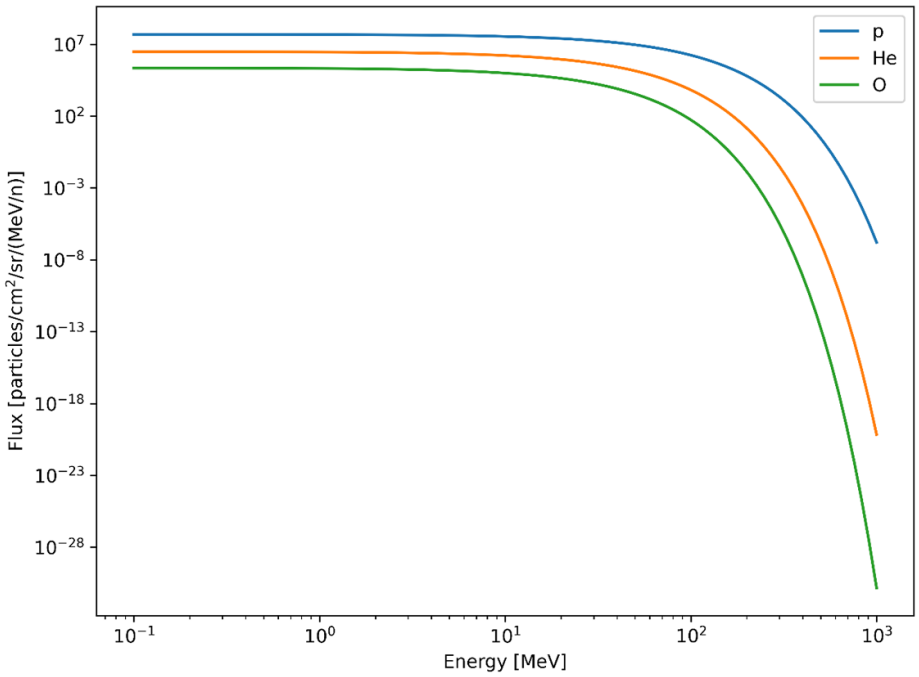

Figure 1. Particle differential flux for the August 1972 SPE.

Table 2. Main characteristics of the ICRP adult male and female reference computational phantoms [28]. Used in this work.

Property	Male	Female
Height (m)	1.76	1.63
Mass (kg)	73	60
Number of tissue voxels	1946 375	3886 020
Slice thickness (voxel height, mm)	8.0	4.84
Voxel in-plane resolution (mm)	2.137	1.775
Voxel volume (mm^3)	36.54	15.25
Number of columns	254	299
Number of rows	127	137
Number of slices	220	346

The main characteristics of these two phantoms are summarized in table 2, whereas table 3 shows a list of phantom regions together with their segmented volumes and resulting masses. Figure 2 shows the male phantom implemented in FLUKA.

The postprocessing of the FLUKA simulations was performed using Python, to calculate the dose in each organ.

3. Results and discussion

3.1. Absorbed doses

Table 4 reports the calculated absorbed doses in different organs of the male and female phantom described in section 2.3 behind a 0.3 g cm^{-2} Al shielding, which is representative of a (light) spacesuit.

For most organs the female dose is higher than the corresponding male dose, mainly due to reduced body size and thus reduced self-shielding. Concerning the tissues/organs usually considered for non-cancer effects (skin, BFO, eye, heart and CNS), little difference was found for skin and BFO (for which the female dose was only 5% and 4% higher than the male dose, respectively), but larger differences were shown by eye (female dose 30% higher than male dose), heart (female dose 24% higher than male dose) and brain (female dose 14% higher than male dose). The organs showing the largest differences were bladder (female dose ∼2.5 times higher than male dose), pancreas (factor ∼2.0) and spleen (factor ∼1.4). Other organs with female dose higher than the male dose were liver (female dose 32% higher than male), oral mucosa (25%), stomach (24%), lung (22%) and small intestine (20%).

Table 3. List of phantom regions, with their segmented volumes and resulting masses.

	Male		Female	
	Volume (cm^3)	Mass (g)	Volume (cm^3)	Mass (g)
Adrenals	13.6	14	12.6	13
Blood (segmented vessels)*	973.7	1032.1	807.4	855.8
Brain	1381	1450	1238.1	1300
Breast	25.6	25	511.9	500
Eyes	14.3	15	14.3	15
Eye lenses	0.4	0.4	0.4	0.4
Gall bladder	66	68	54.3	56
Stomach wall	144.2	150	134.6	140
Stomach contents	240.4	250	221.2	230
Small intestine wall	625	650	576.9	600
Small intestine contents	336.6	350	269.2	280
Right colon wall	144.2	150	139.4	145
Right colon contents	144.3	150	153.8	160
Left colon wall	144.2	150	139.4	145
Left colon contents	72.1	75	76.9	80
Recto-sigmoid colon wall .	67.3	70	67.3	70
Sigmoid colon contents	72.1	75	76.9	80
Heart	795.4	840	587.2	620
Kidneys	295.3	310	261.9	275
Liver	1714.3	1800	1333.3	1400
Lungs	2891.3	1200	2300.8	950
Lymphatic tissue	134	138	76.8	79.1
Muscle tissue	27 619	29 000	16 666.7	17 500
Oesophagus	38.8	40	34	35
Ovaries			10.6	11
Pancreas	133.3	140	114.3	120
Pituitary gland	0.6	0.6	0.6	0.6
Prostate	16.5	17		
Residual (adipose) tissue	21 535.2	20 458.4	24 838.3	23 596.4
Salivary glands	82.5	85	68	70
Skin	3420.2	3728	2496.8	2721.5
Skeleton	7725.3	10 450	5767.4	7760.1
Spleen	144.2	150	125	130
Teeth	18.2	50	14.6	40
Testes	33.7	35		
Thymus	24.3	25	19.4	20
Thyroid	19.2	20	16.4	17
Tongue	69.5	73	57.1	60
Tonsils	2.9	3	2.9	3
Ureters	15.5	16	14.6	15
Urinary bladder wall	48.1	50	38.5	40
Urinary bladder contents	192.3	200	192.3	200
Uterus			77.7	80

At the same time, for some organs the female dose was lower than the male dose. The largest differences were found for adrenals (male dose about 6 times higher than female dose), Extra-Thoracic regions (male dose ∼1.4 times the female doses), salivary glands (male dose 41% higher than female dose), breast (31%) and lymph nodes (18%); differences of 10% or less were found for thyroid, bone surface, gall bladder, muscle, thymus and blood vessels.

Since these differences are basically related to the body self-shielding, in general they should become less important by increasing the shield thickness. This is confirmed by the results presented in table 5, which reports the same type of information shown in table 4 (i.e. absorbed doses in different male and female organs) behind 20 g cm^{-2} Al shielding.

Analogous to the 0.3 g cm^{-2} case, little difference between male and female was found for skin and BFO, for which the female dose was 4% and 7% higher than the male dose, respectively. Larger differences were found for eye (female dose 12% higher than male dose), heart (17%) and brain (11%); however, these differences were smaller than those reported above for the 0.3 g cm^{-2} case (for which these percentages were 30% for eye, 24% for heart and 14% for brain).

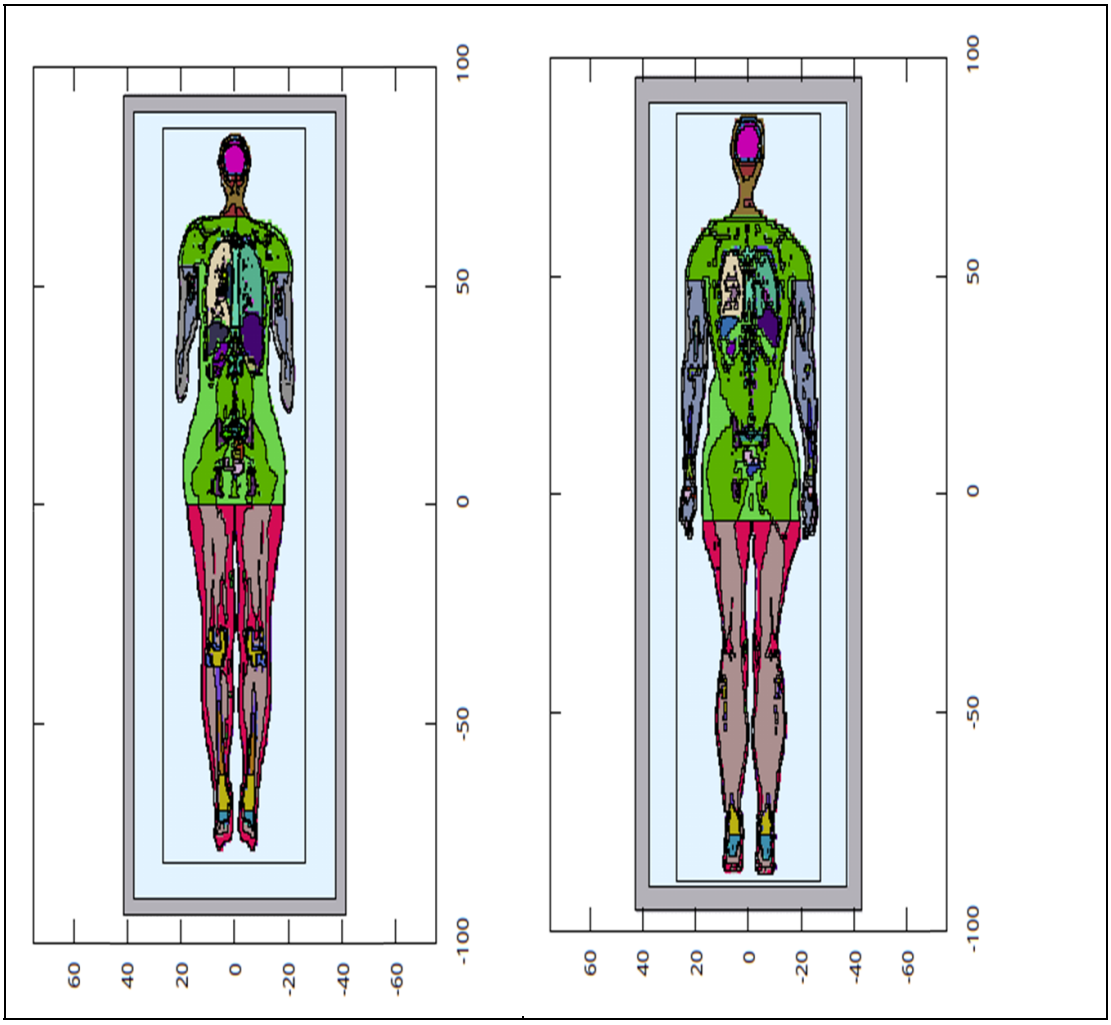

Figure 2. Adult female and male phantoms implemented in FLUKA and used in this work.

By considering all tissues/organs, also at 20 g cm^{-2} large differences were found for bladder (female dose ∼1.4 times higher than male dose), pancreas (factor ∼1.4), liver (factor ∼1.25) and spleen (∼1.2). Again, these differences were smaller than those found at 0.3 g cm^{-2} (for which these factors were 2.5 for bladder, 2.0 for pancreas, 1.3 for liver and 1.4 for spleen). In summary, with the only exception of thyroid and muscles, those organs for which at 0.3 g cm^{-2} the female dose was lower than the male dose, showed closer doses at 20 g cm^{-2}. This can be explained by considering that the differences between male and female doses are related to the body self-shielding, which becomes less important by increasing the Al shielding; therefore, the difference between male and female doses tends to decrease. Of course, this does not hold for tissues/organs for which self-shielding is not important, typically skin, for which the difference between male and female dose was basically the same at 0.3 and 20 g cm^{-2}.

3.2. Gray-Equivalent doses and comparisons with astronauts' dose limits

Table 6 reports the calculated Gy-Eq doses as a function of Al shielding for skin, BFO, eye, heart and CNS.

Since the typical duration of a SPE is a few hours or days, these numbers should be compared with the 30 d limits reported in table 1, that is 1.5 Gy-Eq for skin, 0.25 Gy-Eq for BFO, 1.0 Gy-Eq for eye, 0.25 Gy-Eq for heart and 0.5 Gy-Eq for CNS. This comparison shows that Al shielding values equal or smaller than 5 g cm^{-2} do not allow to respect any of these limits, whereas a 10 g cm^{-2} Al shielding allows respecting all the limits. Similar conclusions were drawn by other researchers who analysed the August 1972 event. For instance, Townsend *et al* [29] calculated organ doses for the female adult voxel phantom and the only exceptions were the BFO dose, which even at 10 g cm^{-2} was slightly above the limit, and the CNS dose, which at 5 g cm^{-2} was already slightly below the limit. Cucinotta *et al* [6] did not report the dose values behind 10 g cm^{-2}, but it is worth mentioning that, according to their calculations for a male phantom exposed to the August 1972 SPE, a 5 g cm^{-2} Al-shielding was not sufficient to respect the organ dose limits, whereas the

Table 4. Absorbed doses (in Gy) in the various organs of the male (M) and female (F) phantom behind 0.3 g cm^{-2} Al shielding.

Organ	M (Gy)	F (Gy)
Skin	14.33	15.07
BFO	1.15	1.20
Colon	0.92	0.93
Lung	0.92	1.12
Stomach	0.59	0.73
Breast	8.17	6.25
Heart	0.57	0.71
Bladder	0.44	1.10
Esophagus	0.60	0.71
Liver	0.69	0.91
Uterus cervix	\	0.34
Ovaries	\	0.31
Testis	3.36	\
Prostate	0.96	\
Thyroid	2.07	1.98
Bone	2.39	2.34
Brain	1.69	1.93
Salivary Glands	4.16	2.95
Adrenals	2.49	0.41
Gallbladder	0.44	0.40
Kidney	0.50	0.56
Lymphatic nodes	1.66	1.40
ET regions	3.61	2.25
Muscle	2.41	2.27
Oral mucosa	1.50	1.87
Pancreas	0.25	0.49
Small intestine	0.54	0.65
Spleen	0.64	0.92
Thymus	1.64	1.47
Blood vessels	2.04	1.89
Lens	9.23	8.42
Eyes	5.10	6.66

organ doses obtained for a 20 g cm^{-2} Al shield were largely below the limits. The considered thicknesses correspond to ranges of protons with initial energies of about 15 MeV (0.3 g cm^{-2}), 30 MeV (1 g cm^{-2}), 40 MeV (2 g cm^{-2}), 70 MeV (5 g cm^{-2}), 100 MeV (10 g cm^{-2}) and 150 MeV (20 g cm^{-2}). Therefore, protons with energies lower than the mentioned values are completely absorbed by the corresponding thicknesses.

3.3. Effective doses

The calculated effective doses for the male and female phantom as a function of the Al shielding in case of an event like the August 1972 SPE are reported in figure 3.

For each considered shielding thickness, the female dose is higher than the male dose. The difference tends to decrease with increasing shielding: while at 0.3 g cm^{-2} shielding the female dose is 29% higher than the male dose, at 20 g cm^{-2} this percentage decreases to 10%. Again, this behaviour can be explained by considering that the role of the body self-shielding tends to become less important by increasing the 'external' shielding. More generally, these numbers confirm that female astronauts may be more at risk than male in case of an intense SPE. This is especially true when the astronauts are protected by a small shielding, such as that provided by the spacesuit, and it should be taken into account in planning the various crew activities. On this subject, it is worth mentioning that during a lunar mission up to 15% of time may be spent in extravehicular activities [6].

Concerning a comparison with the career effective-dose limits, both for male and for female astronauts a 5 g cm^{-2} Al shielding would allow respecting the 1 Sv ESA limit, but this limit would be exceeded with light shielding such as 2 g cm^{-2} or less. Concerning the 0.6 Sv NASA limit, the situation is different for male and female astronauts, because a 5 g cm^{-2} Al shielding would be sufficient for males but not for females. These career limits are intended to protect against the risk of stochastic effects, that is radiation-induced cancer; however, one should also consider that, according to the requirement for the Artemis Orion vehicle, the system shall ensure that effective dose to any crew member does not exceed 0.15 Sv for the design SPE [30]. According to our results, a 10 g cm^{-2} Al shielding does not allow to respect this requirement, whereas a 20 g cm^{-2} Al shielding allows to respect it.

Table 5. Absorbed doses (in Gy) in the various organs of the male (M) and female (F) phantom behind 20 g cm^{-2} Al shielding.

Organ	M (Gy)	F (Gy)
Skin	0.071	0.074
BFO	0.028	0.030
Colon	0.028	0.029
Lung	0.030	0.035
Stomach	0.024	0.028
Breast	0.066	0.063
Heart	0.024	0.028
Bladder	0.021	0.029
Esophagus	0.025	0.028
Liver	0.024	0.030
Uterus cervix	\	0.019
Ovaries	\	0.018
Testis	0.043	\
Prostate	0.031	\
Thyroid	0.043	0.040
Bone	0.039	0.041
Brain	0.037	0.041
Salivary Glands	0.054	0.051
Adrenals	0.042	0.019
Gallbladder	0.021	0.022
Kidney	0.022	0.025
Lymphatic nodes	0.032	0.033
ET regions	0.049	0.045
Muscle	0.041	0.047
Oral mucosa	0.038	0.042
Pancreas	0.016	0.023
Small intestine	0.023	0.025
Spleen	0.024	0.030
Thymus	0.039	0.037
Blood vessels	0.033	0.036
Lens	0.064	0.074
Eyes	0.057	0.064

Table 6. Organ Gy-Eq doses as a function of Al shielding thickness (in g cm^{-2}) for the male (M) and female (F) phantom.

Al shield	Skin-M	Skin-F	BFO-M	BFO-F	Eye-M	Eye-F	Heart-M	Heart-F	CNS-M	CNS-F
0.3	18.40	19.30	1.66	1.71	6.90	8.73	0.82	1.01	2.31	2.61
1	10.18	10.63	1.29	1.35	4.73	5.76	0.70	0.86	1.82	2.06
2	5.95	6.20	0.96	1.01	3.19	3.89	0.57	0.69	1.35	1.53
5	2.07	2.16	0.47	0.50	1.28	1.51	0.32	0.39	0.65	0.74
10	0.63	0.65	0.19	0.20	0.46	0.49	0.15	0.17	0.26	0.29
20	0.125	0.130	0.054	0.058	0.095	0.110	0.049	0.056	0.07	0.08

4. Summary and conclusions

In this work we implemented the ICRP male and female voxel phantoms and we calculated organ-specific absorbed doses and Gy-Eq doses, as well as effective doses, following exposure to the August 1972 SPE under different shielding conditions. For most organs, the female doses were found to be higher than the male doses, basically due to the reduced body self-shielding. This is especially true for light shielding, whereas the difference tends to become less important with heavy shielding. Both for male and for female astronauts, a 10 g cm^{-2} Al-shielding was found to be sufficient to respect all the 30 d-mission organ limits. However, such limits would be exceeded with an Al shielding equal or smaller than 5 g cm^{-2}, which is the case of extra-vehicular activities; especially in that case, the fact that the risk for female astronauts would be significantly higher than for males, should be considered when planning the activities of the various crew members. Furthermore, our calculations showed that a 10 g cm^{-2} Al-shielding would not allow to fulfill the effective-dose design requirement for the Orion vehicle used for the Artemis missions, whereas a 20 g cm^{-2} Al-shielding would allow respecting such requirement. This is consistent with the fact that, in case of an intense SPE, the astronauts should stay in the most heavily shielded part of the vehicle, and should create a shelter using the stowage bags available on board.

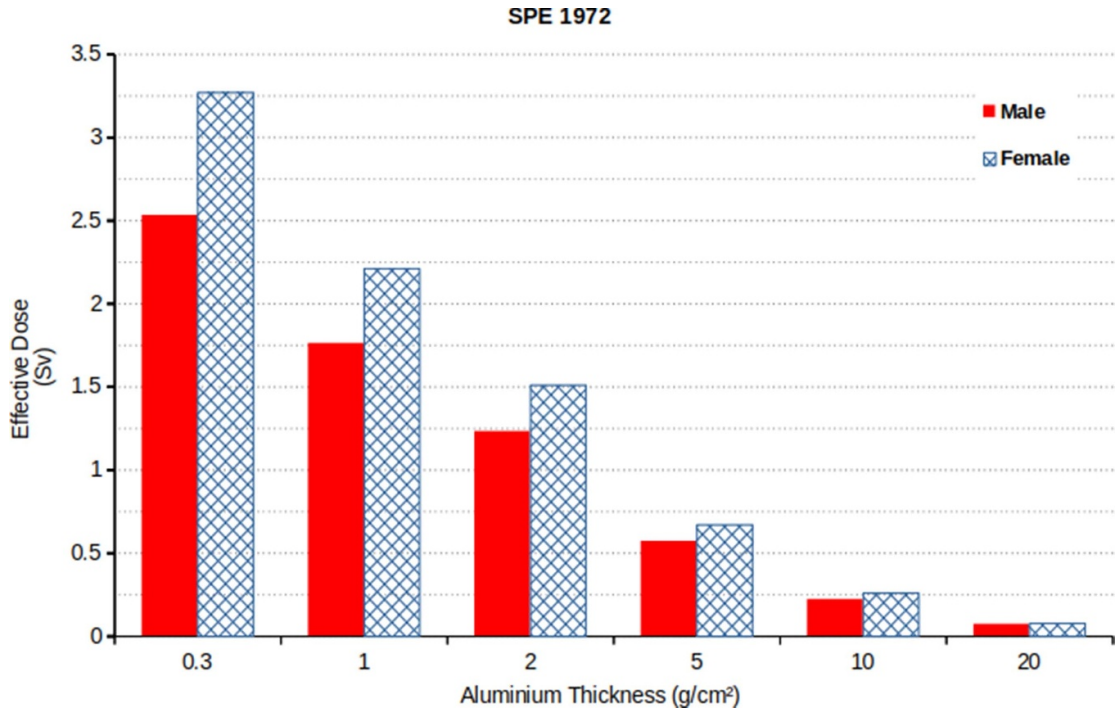

Figure 3. Effective doses (in Sv) as a function of Al shielding for the male and female phantom exposed to the August 1972 SPE.

Data availability statement

The data cannot be made publicly available upon publication because no suitable repository exists for hosting data in this field of study. The data that support the findings of this study are available upon reasonable request from the authors.

Acknowledgments

This work was supported by INFN (CSNV project 'ARES') and by Regione Lombardia (INSpIRIT Project, ID 1161908, co-funded on resources POR FESR 2014-2020-Asse 1).

ORCID iDs

Ricardo Luis Ramos https://orcid.org/0000-0002-1624-7425
Valerio Vercesi https://orcid.org/0000-0001-7670-4563
Francesca Ballarini https://orcid.org/0000-0002-6629-3382

References

[1] Patel S 2020 The effects of microgravity and space radiation on cardiovascular health: from low-Earth orbit and beyond *Int. J. Cardiol. Heart Vasc.* **30** 100595
[2] Durante M and Cucinotta F A 2011 Physical basis of radiation protection in space travel *Rev. Mod. Phys.* **83** 1245
[3] Simonsen L C, Slaba T C, Guida P and Rusek A 2020 NASA's first ground-based galactic cosmic ray simulator: enabling a new era in space radiobiology research *PLoS Biol.* **18** e3000669
[4] Ramos R L, Carante M P, Ferrari A, Sala P, Vercesi V and Ballarini F 2023 A mission to Mars: prediction of GCR doses and comparison with the astronauts' dose limits *Int. J. Mol. Sci.* **24** 2328
[5] NASA regulations 2022 *2022–01-05-NASA-STD-3001* vol 1 *2022–01-05-NASA-STD-3001*
[6] Cucinotta F A 2010 Radiation risk acceptability and limitations (available at: https://three.jsc.nasa.gov/articles/astronautradlimitsfc.pdf)
[7] Durante M and Cucinotta F A 2008 Heavy ion carcinogenesis and human space exploration *Nat. Rev. Cancer* **8** 465–72
[8] NCRP 2000 *Radiation Protection Guidance for Activities in Low-Earth Orbit NCRP Report No. 132* (NCRP)
[9] Cucinotta F A 1999 Issues in risk assessment from solar particle events *Radiat. Meas.* **30** 261–8
[10] Kim M-H Y, Wilson J W, Cucinotta F A, Simonsen L C, Atwell W, Badavi F F and Miller J 1999 Contribution of high charge and energy (HZE), ions during solar-particle event of September 29 1989 *NASA TP- 209320*
[11] Wilson J W, Cucinotta F A, Shinn J, Simonsen L, Dubey R D, Jordon W R, Jones J D, Chang C K and Kim M Y 1999 Shielding from solar particle event exposures in deep space *Radiat. Meas.* **30** 361–82
[12] Parsons J L and Townsend L W 2000 Interplanetary crew dose rates for the August 1972 solar particle event *Radiat. Res.* **153** 729–33

[13] Ballarini F et al 2006 GCR and SPE organ doses in deep space with different shielding: Monte Carlo simulations based on the FLUKA code coupled to anthropomorphic phantoms *Adv. Space Res.* **37** 1791–7
[14] Ramos R L, Carante M P, Bernardini E, Ferrari A, Sala P, Vercesi V and Ballarini F 2024 A method to predict space radiation biological effectiveness for non-cancer effects following intense solar particle events *Life Sci. Space Res.* **41** 210–7
[15] Ballarini F and Carante M P 2016 Chromosome aberrations and cell death by ionizing radiation: evolution of a biophysical model *Radiat. Phys. Chem.* **128C** 18–25
[16] Carante M P, Aimè C, Tello Cajiao J J and Ballarini F 2018 BIANCA, a biophysical model of cell survival and chromosome damage by protons, C-ions and He-ions at energies and doses used in hadrontherapy *Phys. Med. Biol.* **63** 075007
[17] Hall E and Giaccia A 2012 *Radiobiology for the Radiologist* 7th edn (Lippincott Williams & Wilkins)
[18] Ferrari A, Sala P R, Fassò A and Ranft J 2005 FLUKA: a multi-particle transport code *CERN 2005–10, INFN/TC_05/11, SLAC-R-773*
[19] Bohlen T T, Cerutti F, Chin M P W, Fassò A, Ferrari A, Ortega P G, Mairani A, Sala P, Smirnov G and Vlachoudis V 2014 The FLUKA code: developments and challenges for high energy and medical applications *Nucl. Data Sheets* **120** 211–4
[20] Aiginger H et al 2005 The FLUKA code: new developments and application to 1 GeV/n iron beams *Adv. Space Res.* **35** 214–2222005
[21] Carante M P, Aricò G, Ferrari A, Kozlowska W, Mairani A and Ballarini F 2019 First benchmarking of the BIANCA model for cell survival predictions in a clinical hadron therapy scenario *Phys. Med. Biol.* **64** 215008
[22] Ramos R L, Embriaco A, Carante M P, Ferrari A, Sala P, Vercesi V and Ballarini F 2022 Radiobiological damage by space radiation: extension of the BIANCA model to heavy ions up to Iron, and pilot application to cosmic ray exposure *J. Radiol. Prot.* **42** 021523
[23] Carante M P, Aricò G, Ferrari A, Karger C, Kozlowska W, Mairani A, Sala P and Ballarini F 2020 In vivo validation of the BIANCA biophysical model: benchmarking against rat spinal cord RBE data *Int. J. Mol. Sci.* **21** 3973
[24] Carante M P, Embriaco A, Aricò G, Ferrari A, Mairani A, Mein S, Ramos R, Sala P and Ballarini F 2021 Biological effectiveness of He-3 and He-4 ion beams for cancer hadrontherapy: a study based on the BIANCA biophysical model *Phys. Med. Biol.* **66** 195009
[25] Embriaco A, Ramos R L, Carante M P, Ferrari A, Sala P, Vercesi V and Ballarini F 2021 Healthy tissue damage following cancer ion therapy: a radiobiological database predicting lymphocyte chromosome aberrations based on the BIANCA biophysical model *Int. J. Mol. Sci.* **22** 10877
[26] Kozlowska W, Carante M, Aricò G, Ferrari A, Magro G, Mairani A, Sala P, Georg D and Ballarini F 2022 First application of the BIANCA model to carbon-ion patient cases *Phys. Med. Biol.* **67** 115013
[27] Bertsch D, Biswas S and Reames D 1974 Observation of cosmic gamma radiation above 10 MeV *Sol. Phys.* **39** 479–91
[28] ICRP 2009 Adult reference computational phantoms (ICRP Publication 110. Ann. ICRP) vol 39
[29] Townsend L, Zaman F and de Wet W Estimates of radiation exposures to crews on missions in cis-lunar space and on the lunar surface from the August 1972 SEP event 49th *Int. Conf. Environmental Systems* (*Massachusetts*, 7–11 July 2019)
[30] Townsend L W et al 2018 Solar particle event storm shelter requirements for missions beyond low Earth orbit *Life Sci. Space Res.* **17** 32–39